

propyl structures, has its P–C11–C12–C13 torsion angle in the lower-energy *trans* conformation, it is probable that the *gauche* P1–C111–C112–C113 torsion angle is a crystal packing phenomena and that it is the extended conformation which is required for biological activity. This is in agreement with the suggestion by Czerwinski & Ponnuswamy (1988a) that the conformation of the substituted moieties is the primary cause of the biological activity. However, it may be that the presence of a positive charge at the end of this extended hydrophobic chain and/or the length of the alkyl chain is the predominant factor in determining the biological effectiveness of the compound. Structure determinations of other active and inactive compounds in this series are currently underway to resolve this question.

The title compound was a gift from Dr G. R. Hillman, Department of Pharmacology and Toxicology, The University of Texas Medical Branch. Research supported by The Robert A. Welch Foundation (H-779) and NIH Biomedical Research Support Grant RR 7205.

References

- ARCHER, S. J., MODRO, T. A. & NASSIMBENI, L. R. (1981). *Phosphorus Sulfur*, **11**, 101–110.
- BART, J. C. J., BASSI, I. W. & CALCATERRA, M. (1980). *J. Organomet. Chem.* **193**, 1–12.
- BART, J. C. J., BASSI, I. W. & CALCATERRA, M. (1981). *Phosphorus Sulfur*, **9**, 347–352.
- CZERWINSKI, E. W. (1986). *Acta Cryst.* **C42**, 236–239.
- CZERWINSKI, E. W. & PONNUSWAMY, M. N. (1988a). *Acta Cryst.* **C44**, 862–865.
- CZERWINSKI, E. W. & PONNUSWAMY, M. N. (1988b). *Acta Cryst.* **C44**, 1862–1864.
- EISENBERG, D. & CROTHERS, D. (1979). *Physical Chemistry with Applications to the Life Sciences*. Menlo Park: Benjamin/Cummings.
- FRENZ, B. A. (1985). *Enraf–Nonius SDP-Plus Structure Determination Package*. Version 3.0. Enraf–Nonius, Delft, The Netherlands.
- GOLDSTEIN, B. M., TAKUSAGAWA, F., SRIVASTAVA, P. C. & KNAPP, F. F. JR (1986). *Acta Cryst.* **C42**, 570–573.
- HENICHART, J. P., HOUSSIN, R., VACCHER, C., FOULON, M. & BAERT, F. (1983). *J. Mol. Struct.* **99**, 283–293.
- International Tables for X-ray Crystallography* (1974). Vol. IV, Tables 2.2B and 2.3.1. Birmingham: Kynoch Press. (Present distributor Kluwer Academic Publishers, Dordrecht.)
- KOVACS, T. & PARKANYI, L. (1982). *Cryst. Struct. Commun.* **11**, 1565–1570.
- MCALLISTER, P. R., DOTSON, M. J., GRIM, S. O. & HILLMAN, G. R. (1980). *J. Med. Chem.* **23**, 862–865.
- PONNUSWAMY, M. N. & CZERWINSKI, E. W. (1986). *Acta Cryst.* **C42**, 1019–1022.
- SKAPSKI, A. C. & STEPHENS, F. A. (1974). *J. Cryst. Mol. Struct.* **4**, 77–85.
- STOUT, G. H. & JENSEN, L. H. (1968). In *X-ray Structure Determination*. New York: Macmillan.
- WALKER, N. & STUART, D. (1983). *Acta Cryst.* **A39**, 158–166.

Acta Cryst. (1989). **C45**, 1039–1044

Structural and Molecular Orbital Study of Ergoline Derivatives. Ethyl 2(*S*)- and 2(*R*)-Cyano-2-(6-methylergolin-8 β -yl)methylbutyrate

BY E. FORESTI AND P. SABATINO

Dipartimento di Chimica G. Ciamician, Università di Bologna, 40126 Bologna, Italy

L. RIVA DI SANSEVERINO

Dipartimento di Scienze Mineralogiche, Università di Bologna, 40126 Bologna, Italy

C. TOSI AND R. FUSCO

Istituto Guido Donegani, 28100 Novara, Italy

AND R. TONANI

Farmitalia Carlo Erba, 20146 Milano, Italy

(Received 9 September 1988; accepted 19 December 1988)

Abstract. (I): C₂₃H₂₉N₃O₂, m.p. 510–512 K, $M_r = 379.5$, monoclinic, $P2_1$, $a = 6.189$ (2), $b = 13.211$ (2), $c = 12.855$ (2) Å, $\beta = 102.76$ (2)°, $V = 1025.1$ (4) Å³, $Z = 2$, $D_x = 1.22$ Mg m⁻³, graphite-monochromatized

Mo K α radiation ($\lambda = 0.71069$ Å), $\mu = 0.07$ mm⁻¹, $F(000) = 408$, $T = 293$ K, final $R = 0.047$ for 1626 independent reflections. (II): C₂₃H₂₉N₃O₂, m.p. 496–498 K, $M_r = 379.5$, monoclinic, $P2_1$, $a = 6.224$ (1),

0108-2701/89/071039-06\$03.00

© 1989 International Union of Crystallography

$b = 12.741$ (1), $c = 13.609$ (2) Å, $\beta = 102.56$ (1)°, $V = 1053.4$ (2) Å³, $Z = 2$, $D_x = 1.19$ Mg m⁻³, graphite-monochromatized Mo $K\alpha$ radiation ($\lambda = 0.71069$ Å), $\mu = 0.07$ mm⁻¹, $F(000) = 408$, $T = 293$ K, final $R = 0.046$ for 1013 independent reflexions. The two epimers (I) and (II) have opposite chirality at the C19 centre, and different pharmacological activity on dopamine (DA) and serotonin receptors. Theoretical investigations, carried out with quantum- and molecular-mechanical methods, suggest that different binding affinities for the receptors are related to spatial differences of the charge distribution in the two molecules, as evidenced by both the electrostatic potential maps and the observed torsion angles along the side chain at C8.

Introduction. Ergoline derivatives constitute an important class of molecules acting on the central nervous system, which exhibit various kinds and degrees of activity on DA, adrenaline and serotonin receptors (Bernardi, 1987). The two epimers (I) and (II) are active on D₂ and 5HT₂ receptors of DA and serotonin, compound (II) showing a higher degree of affinity towards DA than (I).

In order to study the influence of structure on pharmacological behaviour, both the X-ray single-crystal analysis and a theoretical investigation of the conformational properties of (I) and (II) were performed. The good agreement between the results of the two approaches shows that computer-aided molecular modelling techniques can be a useful tool for the prediction of the preferred molecular conformation for the entire family of synthetic ergoline derivatives synthesized by Farmitalia Carlo Erba Laboratories with the aim of mimicking the pharmacological profile of ergot alkaloids.

Experimental. Crystals synthesized (Mantegani, Arcari, Caravaggi & Bosisio, 1982) as transparent plates from ethanol [(I), dimensions 0.31 × 0.14 × 0.48 mm] and from methylene chloride [(II), dimensions 0.20 × 0.15 × 0.05 mm]. Cell parameters from 23 reflections ($11 \leq \theta \leq 14^\circ$) for (I), from 25 reflections ($8 \leq \theta \leq 11^\circ$) for (II), on an Enraf-Nonius CAD-4 diffractometer.

(I). $\omega/2\theta$ scan, $2\theta_{\max} = 54^\circ$, scan speed from 0.5 to 8° min⁻¹, scan range $0.8^\circ + 0.35^\circ \tan\theta$, background measured in stationary mode, 0.5 times the peak scan time, 2325 reflections measured ($h = 0, 7; k = 0, 16; l = -16, 16$), 1976 unique ($R_{\text{int}} = 0.01$), 1626 with $I > [2.5\sigma(I)]$, three standard reflections (235, 171 and 351), no significant intensity variation, no absorption or extinction corrections applied.

(II). $\omega/2\theta$ scan, $2\theta_{\max} = 50^\circ$, scan speed from 0.6 to 5° min⁻¹, scan range $0.7^\circ + 0.35^\circ \tan\theta$, background measured in stationary mode, 0.5 times the peak scan time, 2024 reflections measured ($h = -7, 7; k = 0, 15; l = 0, 16$), 1693 unique ($R_{\text{int}} = 0.023$), 1013 with

Table 1. Fractional atomic coordinates and thermal parameters (Å²) of (I)

$U_{\text{eq}} = \frac{1}{3}$ trace of the orthogonalized U_{ij} matrix.

	<i>x</i>	<i>y</i>	<i>z</i>	U_{iso} or U_{eq}
N1	0.6972 (5)	0.4320 (3)	0.0064 (3)	0.049 (1)
C2	0.5657 (6)	0.3720 (4)	-0.0714 (3)	0.047 (1)
C3	0.4411 (5)	0.3077 (3)	-0.0255 (3)	0.040 (1)
C4	0.2716 (6)	0.2260 (4)	-0.0655 (3)	0.041 (1)
C5	0.1305 (5)	0.2041 (4)	0.0171 (3)	0.037 (1)
N6	-0.0008 (5)	0.1105 (3)	-0.0118 (2)	0.039 (1)
C7	-0.1446 (5)	0.0899 (4)	0.0633 (3)	0.042 (1)
C8	-0.0135 (5)	0.0740	0.1768 (3)	0.039 (1)
C9	0.1310 (6)	0.1659 (4)	0.2113 (3)	0.042 (1)
C10	0.2725 (5)	0.1903 (3)	0.1315 (3)	0.036 (1)
C11	0.4238 (5)	0.2793 (4)	0.1660 (3)	0.040 (1)
C12	0.5054 (6)	0.3139 (4)	0.2690 (3)	0.050 (1)
C13	0.6596 (7)	0.3934 (4)	0.2882 (4)	0.061 (1)
C14	0.7380 (6)	0.4391 (4)	0.2074 (3)	0.056 (1)
C15	0.6551 (6)	0.4054 (4)	0.1035 (3)	0.045 (1)
C16	0.4980 (6)	0.3285 (4)	0.0847 (3)	0.040 (1)
C17	-0.1448 (6)	0.1155 (4)	-0.1195 (3)	0.049 (1)
C18	-0.1769 (5)	0.0534 (4)	0.2490 (3)	0.044 (1)
C19	-0.0766 (5)	0.0213 (4)	0.3653 (3)	0.043 (1)
C20	0.0302 (6)	0.1105 (4)	0.4310 (3)	0.051 (1)
O21	-0.0702 (5)	0.1870 (3)	0.4378 (2)	0.072 (1)
O22	0.2421 (4)	0.0953 (3)	0.4797 (2)	0.058 (1)
C23	0.3641 (8)	0.1808 (5)	0.5375 (4)	0.081 (1)
C24 (1)*	0.3408 (11)	0.1824 (7)	0.6507 (5)	0.099 (2)
C24(2)	0.5073 (15)	0.1560 (13)	0.6447 (9)	0.062 (2)
C25	0.0809 (6)	-0.0614 (4)	0.3657 (3)	0.052 (1)
N26	0.1977 (6)	-0.1271 (4)	0.3613 (4)	0.084 (1)
C27	-0.2696 (6)	-0.0173 (4)	0.4140 (3)	0.058 (1)
C28	-0.2064 (8)	-0.0428 (5)	0.5321 (4)	0.079 (1)

* Coordinates of the most populated fraction.

$I > [2.5\sigma(I)]$, three standard reflections (035, 151 and 200), no significant intensity variation, no absorption or extinction corrections applied.

Both structures were solved using the program *MITHRIL* (Gilmore, 1983) which allowed the location of most heavy atoms, while the remainder were found on a difference Fourier map. Full-matrix refinement based on F by least-squares methods was performed using the *SHELX76* system (Sheldrick, 1976). The majority of H atoms were found on difference Fourier maps (the others were located by geometrical calculation) and isotropically refined using a 'riding model' with adequate bond and angle constraints and two different temperature factors for the methylic and the remaining H atoms.

Number of parameters refined: 271 for (I) and 263 for (II). Values of $R = 0.047$, $wR = 0.049$ with $w = 2.7146/[\sigma^2(F_o) + 0.000201(F_o^2)]$ for (I), and $R = 0.046$, $wR = 0.049$ with $w = 2.0592/[\sigma^2(F_o) + 0.000674(F_o^2)]$ (II). Atomic scattering factors taken from *SHELX76*. Max. $\Delta/\sigma = 0.4$ for (I) and 0.2 for (II), both referring to thermal parameters. Maximum positive and negative electron density in final difference Fourier maps 0.26 and -0.17 e Å⁻³ for (I) and 0.19 and -0.18 e Å⁻³ for (II).

In compound (I) an unusually high temperature factor relative to C24 led us to think of possible static disorder; this was confirmed by the appearance of a

Table 2. Fractional atomic coordinates and thermal parameters (\AA^2) for (II)

$U_{eq} = \frac{1}{3}$ trace of the orthogonalized U_{ij} matrix.

	x	y	z	U_{iso} or U_{eq}
N1	0.3074 (9)	0.1507	-0.0168 (4)	0.048 (1)
C2	0.4385 (11)	0.0858 (7)	0.0535 (5)	0.045 (2)
C3	0.5583 (10)	0.0206 (7)	0.0065 (5)	0.042 (2)
C4	0.7241 (12)	-0.0640 (8)	0.0411 (5)	0.047 (2)
C5	0.8700 (10)	-0.0828 (7)	-0.0376 (5)	0.035 (2)
N6	0.9969 (9)	-0.1802 (6)	-0.0137 (4)	0.042 (1)
C7	1.1391 (12)	-0.1995 (8)	-0.0859 (5)	0.049 (2)
C8	1.0154 (11)	-0.2100 (7)	-0.1934 (5)	0.043 (2)
C9	0.8757 (12)	-0.1117 (8)	-0.2213 (5)	0.050 (2)
C10	0.7284 (11)	-0.0915 (7)	-0.1462 (5)	0.039 (2)
C11	0.5812 (12)	0.0017 (8)	-0.1740 (5)	0.049 (2)
C12	0.5023 (13)	0.0426 (8)	-0.2703 (6)	0.064 (2)
C13	0.3477 (13)	0.1277 (9)	-0.2840 (7)	0.074 (3)
C14	0.2667 (13)	0.1710 (8)	-0.2053 (6)	0.064 (2)
C15	0.3464 (10)	0.1266 (7)	-0.1099 (5)	0.044 (2)
C16	0.4996 (11)	0.0476 (7)	-0.0964 (5)	0.041 (2)
C17	1.1398 (11)	-0.1791 (8)	0.0878 (5)	0.048 (4)
C18	1.1806 (13)	-0.2267 (7)	-0.2594 (5)	0.052 (5)
C19	1.1017 (12)	-0.2824 (7)	-0.3606 (6)	0.053 (5)
C20	1.0408 (16)	-0.3943 (9)	-0.3398 (7)	0.067 (6)
O21	1.1580 (12)	-0.4519 (7)	-0.2841 (5)	0.089 (5)
O22	0.8462 (13)	-0.4196 (7)	-0.3938 (8)	0.132 (7)
C23	0.7989 (28)	-0.5334 (8)	-0.4041 (13)	0.189 (19)
C24	0.6492 (26)	-0.5566 (12)	-0.3303 (13)	0.161 (15)
C25	0.9217 (15)	-0.2283 (9)	-0.4260 (6)	0.060 (5)
N26	0.7840 (15)	-0.1833 (9)	-0.4801 (6)	0.089 (6)
C27	1.2985 (13)	-0.2895 (9)	-0.4159 (6)	0.070 (6)
C28	1.2511 (18)	-0.3467 (11)	-0.5136 (8)	0.101 (8)

small peak ($0.35 e \text{\AA}^{-3}$), at a distance of 1.1\AA from C24, in the final stages of the difference maps. By refining both positions the occupancies converged to 0.8 and 0.2, respectively.

Programs *XANADU* (Roberts & Sheldrick, 1975) and *SCHAKAL* (Keller, 1984) were used for geometrical calculations and graphics.

Atomic coordinates are reported in Tables 1 and 2. Bond distances and bond angles, given in Table 3,* are comparable and similar to values found in analogues.

Fig. 1 shows a plot of each compound, together with the atom labelling.

The crystal packing of both (I) and (II) is determined by van der Waals interactions and an intermolecular hydrogen bond, $N1 \cdots N6^{ii}$, $3.005 (5) \text{\AA}$ in (I) and $2.956 (8) \text{\AA}$ in (II), where $(ii) = 1 - x, 0.5 + y, -z$. The hydrogen-bond angle is 161 and 173° in (I) and (II) respectively.

Theoretical calculations. Analogously to our previous work on ergolines (Foresti, Sabatino, Riva di Sanseverino, Fusco, Tosi & Tonani, 1988), X-ray analysis was accompanied by a theoretical investigation of the conformational-energy surface of isolated molecules.

* Lists of structure factors, anisotropic thermal parameters and H-atom coordinates have been deposited with the British Library Document Supply Centre as Supplementary Publication No. SUP 51699 (21 pp.). Copies may be obtained through The Executive Secretary, International Union of Crystallography, 5 Abbey Square, Chester CH1 2HU, England.

Table 3. Bond distances (\AA) and angles ($^\circ$)

	(I)	(II)	(I)	(II)
N1—C2	1.390 (5)	1.388 (8)	C2—N1—C15	108.0 (3) 107.8 (6)
C2—C3	1.367 (5)	1.364 (9)	N1—C2—C3	109.9 (4) 109.8 (6)
C3—C4	1.513 (5)	1.496 (9)	C2—C3—C4	135.3 (4) 134.5 (7)
C4—C5	1.544 (5)	1.566 (9)	C2—C3—C16	105.8 (3) 105.5 (6)
C5—N6	1.481 (5)	1.469 (8)	C4—C3—C16	118.8 (3) 120.0 (6)
C5—C10	1.548 (5)	1.551 (9)	C3—C4—C5	110.8 (3) 111.0 (6)
N6—C7	1.475 (5)	1.479 (9)	C4—C5—N6	110.3 (3) 110.0 (5)
C7—C8	1.519 (5)	1.504 (9)	C4—C5—C10	112.8 (3) 111.7 (5)
C8—C9	1.515 (4)	1.525 (9)	N6—C5—C10	107.7 (3) 108.5 (5)
C9—C10	1.522 (5)	1.536 (9)	C5—N6—C7	111.5 (3) 111.3 (5)
C10—C11	1.507 (5)	1.496 (9)	C5—N6—C17	112.5 (3) 112.7 (5)
C11—C12	1.387 (5)	1.397 (9)	C7—N6—C17	107.2 (3) 107.3 (5)
C12—C13	1.404 (6)	1.435 (8)	N6—C7—C8	112.5 (3) 114.0 (6)
C13—C14	1.379 (6)	1.393 (9)	C7—C8—C9	109.0 (3) 108.3 (6)
C14—C15	1.394 (5)	1.404 (9)	C7—C8—C18	108.7 (3) 108.5 (6)
C15—C16	1.390 (5)	1.371 (9)	C9—C8—C18	112.9 (3) 113.0 (6)
C3—C16	1.409 (5)	1.411 (9)	C8—C9—C10	111.3 (3) 111.2 (6)
C11—C16	1.392 (5)	1.396 (9)	C5—C10—C9	112.0 (3) 110.4 (5)
N6—C17	1.473 (4)	1.471 (9)	C5—C10—C11	111.9 (3) 111.9 (5)
C8—C18	1.540 (5)	1.520 (9)	C9—C10—C11	112.3 (3) 112.7 (6)
C18—C19	1.546 (5)	1.533 (8)	C10—C11—C12	127.5 (3) 127.1 (7)
C19—C20	1.514 (6)	1.518 (8)	C10—C11—C16	115.5 (3) 116.5 (6)
C20—O21	1.199 (5)	1.185 (8)	C12—C11—C16	116.8 (3) 116.2 (7)
C20—O22	1.338 (4)	1.313 (9)	C11—C12—C13	120.3 (4) 119.6 (8)
O22—C23	1.466 (6)	1.480 (6)	C12—C13—C14	122.3 (4) 122.9 (9)
C23—C24	1.494 (7)	1.540 (6)	C13—C14—C15	117.7 (4) 115.9 (8)
C19—C25	1.463 (6)	1.445 (8)	N1—C15—C14	133.2 (4) 131.6 (7)
C25—N26	1.139 (5)	1.153 (9)	N1—C15—C16	107.1 (3) 107.3 (6)
C19—C27	1.552 (5)	1.574 (7)	C14—C15—C16	119.7 (4) 121.0 (7)
C27—C28	1.520 (6)	1.488 (8)	C3—C16—C11	127.7 (3) 126.2 (7)
			C3—C16—C15	109.2 (3) 109.5 (6)
			C11—C16—C15	126.0 (3) 124.3 (7)
			C8—C18—C19	117.0 (3) 118.0 (8)
			C18—C19—C20	111.0 (3) 108.2 (7)
			C18—C19—C25	109.5 (3) 112.7 (6)
			C20—C19—C25	111.8 (3) 111.8 (7)
			C18—C19—C27	107.4 (3) 109.0 (6)
			C20—C19—C27	108.1 (3) 106.7 (7)
			C25—C19—C27	108.9 (3) 108.2 (6)
			C19—C20—O21	121.8 (3) 123.9 (9)
			C19—C20—O22	114.0 (4) 111.3 (9)
			O21—C20—O22	124.2 (4) 124.8 (9)
			C20—O22—C23	117.6 (4) 115.7 (9)
			O22—C23—C24	110.8 (5) 105.2 (6)
			C19—C25—N26	176.7 (5) 177.3 (9)
			C19—C27—C28	115.1 (3) 115.6 (7)

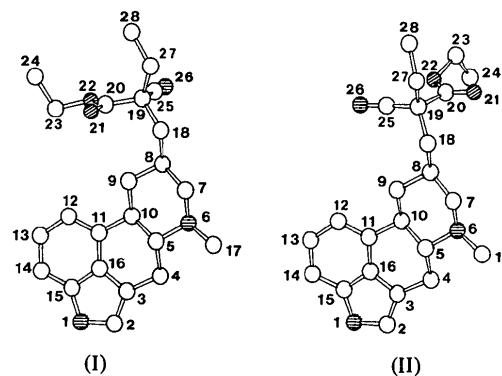


Fig. 1. *SCHAKAL* plot and numbering scheme for (I) and for (II). H atoms have been omitted for clarity.

To carry out this investigation, both quantum mechanical semi-rigorous methods (PCILOPT; Fantucci & Tosi, 1981) and molecular mechanics calculations (LECSA or Low-Energy Conformational Space

Analysis; Fusco, Caccianotti & Tosi, 1986), with the potential-energy functions of Hopfinger (1973), were applied. We briefly recollect here that LECSA aims at an exhaustive sampling of low-energy minima through a 'random search plus local optimization' technique, whereby low-lying minima are uncovered by carrying out a number of energy minimizations starting from random initial sets of the internal rotation angles.

During PCILOPT energy minimizations, all nine possible internal rotations [φ_1 (about N6–C17), φ_2 (C8–C18), φ_3 (C18–C19), φ_4 (C19–C20), φ_5 (C20–O22), φ_6 (O22–C23), φ_7 (C23–C24), φ_8 (C19–C27) and φ_9 (C27–C28)] were changed, while when exploring the low-energy regions of the conformational space with LECSA the three torsions defining the methyl H-atom positions (φ_1 , φ_7 and φ_9) were kept fixed. Bond lengths and angles were held constant at their crystallographic values.

The energy gain on passing from the crystal conformation to the corresponding PCILOPT energy minima is small [2.5 kJ mol⁻¹ for (I) and 8.4 kJ mol⁻¹

for (II)], and also the maximum angular variation is modest [13° for φ_6 in (I) and 21° for φ_3 in (II), see Table 4].

By applying the LECSA algorithm a large number of low-energy minima were detected: 228 for (I) and 162 for (II), in a range of 20 kJ mol⁻¹ above the lowest minimum. The energy of the crystal conformers (C) exceeds the energy of the corresponding lowest minima by 6.2 kJ mol⁻¹ in (I) and 19.7 kJ mol⁻¹ in (II). Considering the torsion angles, in both compounds φ_2 is \pm synclinal (L) instead of antiperiplanar (C) and φ_6 is \pm anticlinal (L) instead of \pm synclinal (C), while the other internal rotation angles do not differ significantly. This is interesting and prompts investigation of the torsional sub-space defined by φ_2 and φ_6 . Fig. 2 shows the isoenergy contours in the two (φ_2 , φ_6) maps (calculated in steps of 15° by optimizing, at each point, the other four torsions), together with the slowest-ascent pathway connecting C and L. For (I) this path has to overcome a barrier of ca 20 kJ mol⁻¹ at (-135, 135°), and for (II) a barrier of ca 24 kJ mol⁻¹ at (-120, 90°).

Table 4. Relevant torsion angles (°)

	(I)			(II)		
	C	P	L	C	P	L
φ_2 (C7–C8–C18–C19)	172.2	176.6	-86.0	155.6	176.9	-97.0
φ_3 (C8–C18–C19–C20)	74.1	71.5	55.4	-65.1	-61.5	-67.9
φ_4 (C18–C19–C20–O22)	55.2	55.2	53.1	-51.2	-55.5	-40.8
φ_5 (C19–C20–O22–C23)	174.9	174.9	141.5	161.8	177.8	-162.0
φ_6 (C20–O22–C23–C24)	89.5	76.7	-141.1	102.2	105.7	130.1
φ_8 (C18–C19–C27–C28)	-174.3	-177.3	-179.1	177.0	177.1	178.5

C = crystal conformation [average $\sigma = 0.5^\circ$ for (I) and 1.0° for (II)].

P = (relative) minimum-energy conformation reached with PCILOPT starting from C.

L = (probably absolute) minimum-energy conformation detected by LECSA.

Discussion. From the above calculations it may be inferred that both molecules (I) and (II) have a good deal of conformational flexibility which will reflect the ease with which they adapt to the receptor shape. In previous work (Foresti *et al.*, 1988) it was suggested that the orientation in space of the substituents at C8 in the ergoline nucleus could be related to the different affinities for the adrenaline, serotonin and DA receptors within the central nervous system. A further contribution to the understanding of the effect of stereoelectronic differences on activity may be obtained

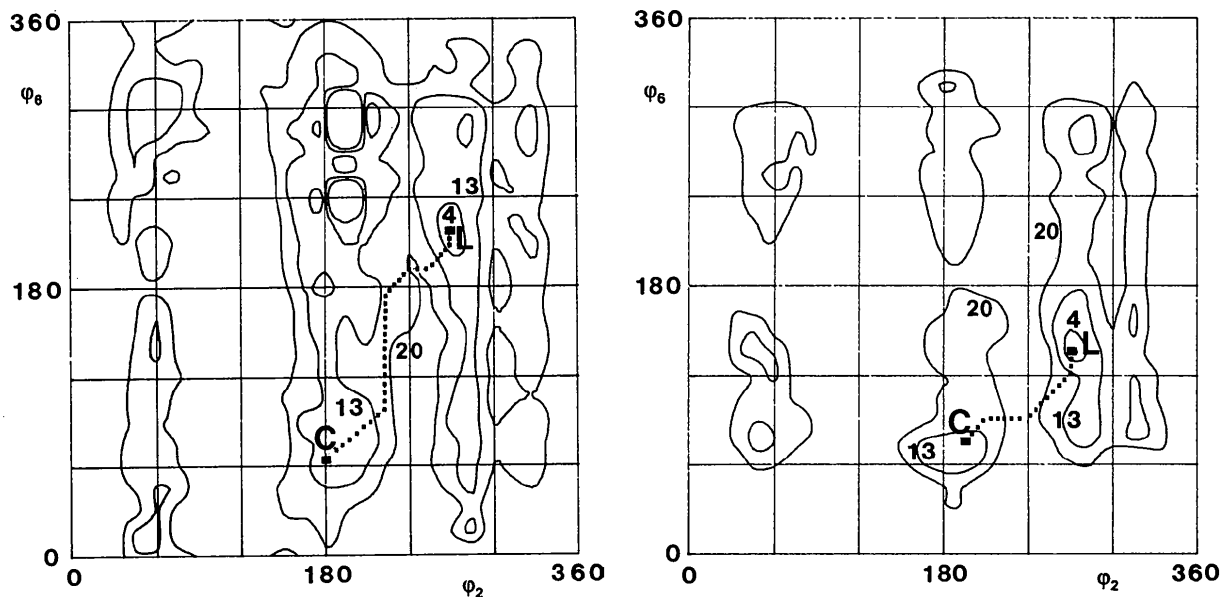


Fig. 2. Isoenergy contour maps for the rotations φ_2 and φ_6 in (I) (left) and (II) (right). Energies are in kJ mol⁻¹.

by studying the maps of the molecular electrostatic potential (MEP) generated around the molecules. These maps are a good reactivity indicator for noncovalent interactions of polar molecules with a common reactant, as it is generally assumed that the early stages of drug-receptor interaction, *i.e.* drug recognition and binding, are driven by long-range electrostatic forces (Weinstein, Chou, Kang, Johnson & Green, 1976). MEP is mainly influenced by the presence of heteroatoms, which may be acceptors or donors of hydrogen

bonds to the active site of the receptor. The different pharmacological activity of congeneric compounds will thus in general be connected to differences in the relative positions of positive and negative regions in the MEP maps. A MEP study of the dopaminergic pharmacophore of ergoline and its analogues (Kocjan, Hodošek & Hadži, 1986) showed that the congruent superimposition of the molecular frameworks obtained between apomorphine (a prototype of dopaminergic drugs) and DA-active ergoline analogues might bear out the assumption that they bind with the same receptor sites when activating certain sub-types of the DA receptor. More recently, a pharmacophore model for attaining D₂ dopaminergic activity was proposed by Tonani, Dunbar, Edmonston & Marshall (1987). Its most important feature is two 'critical' heteroatoms which interact with the receptors: one of these is an N atom while the other can be an O atom (in compounds like dopamine, aminoindanes, 2-aminotetralins, apomorphines) or an N atom (in the natural and synthetic ergolines). In addition to these investigations, the MEP of the catechol moiety of DA was studied, and some pharmacophoric features of DA agonists were proposed (van de Waterbeemd, Carrupt & Testa, 1985).

For the sake of simplicity, the MEP was calculated here in the monopole approximation, making use of our results of Mulliken population analysis from the PCIOPT computation. The MEP maps of (I) and (II), calculated for their crystal conformations in two planes parallel with the plane *xy* defined by N1, C2 and C3 at $z = +1 \text{ \AA}$ and $z = -1 \text{ \AA}$, are shown in Fig. 3. As expected, the maps present common negative and positive regions in correspondence to the tetracyclic ergoline moiety which represents the characteristic structural feature for eliciting biological activity. By contrast, the maps for the two epimers are profoundly different in the region around the chiral centre C19, with a negative region surrounding two positive regions in (I), and a positive region surrounding two negative regions in (II). This implies that the orientation of the C8 substituent drastically affects the binding of the ergoline nucleus to the DA receptor. Clearly the study of MEP maps of other ergoline derivatives is needed to check the actual importance of the differences observed in Fig. 3. Nevertheless, the present structural analysis, revealing defined stereochemical features of the two differently active epimers, contributes further to the hypothesis which assigns a high significance to the topological characteristics of the substituents in eliciting specific drug action.

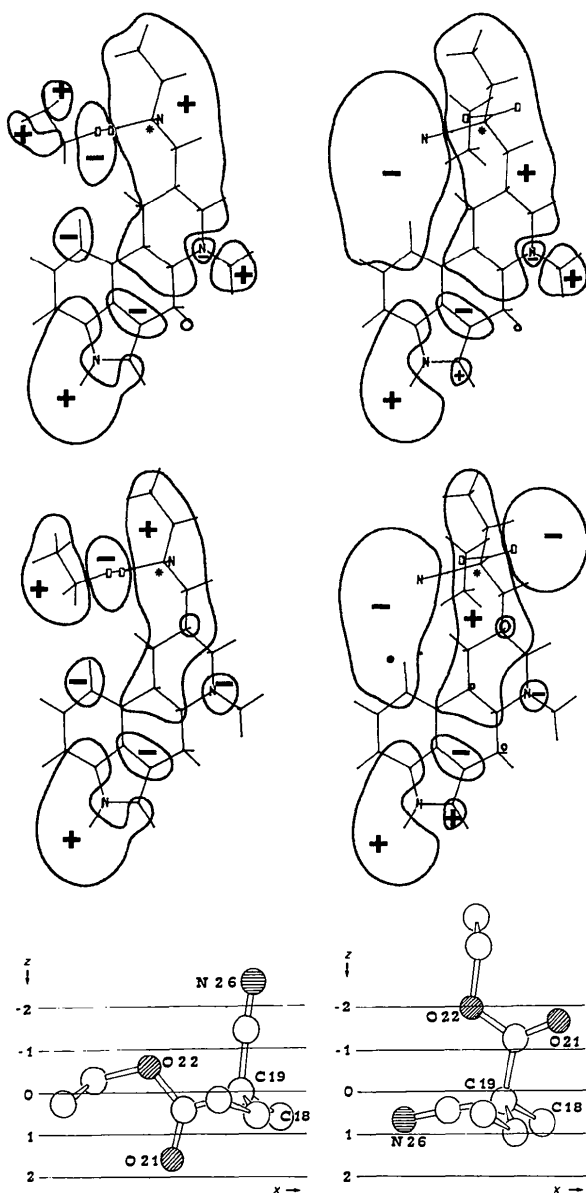


Fig. 3. Molecular electrostatic potential map of (I) (left) and (II) (right), in the planes $z = 1 \text{ \AA}$ (upper) and $z = -1 \text{ \AA}$ (lower). Contour lines correspond to $+10$ and -10 kJ mol^{-1} . The chiral centre C19 is denoted by an asterisk. To aid in the reading of these maps, a projection of the substituents at C8 in the *xz* plane is shown at the bottom.

References

- BERNARDI, L. (1987). Proc. Fr. Ital. Jt Meet. Med. Chem., Pisa, Sept. 22–26, 1987.
 FANTUCCI, P. C. & TOSI, C. (1981). XVI Natl Congr. Ital. Assoc. Phys. Chem., Abstract, p. 33.

- FORESTI, E., SABATINO, P., RIVA DI SANSEVERINO, L., FUSCO, R., TOSI, C. & TONANI, R. (1988). *Acta Cryst. B* **44**, 307–315.
- FUSCO, R., CACCIANOTTI, L. & TOSI, C. (1986). *Nuovo Cimento D*, **8**, 211–217.
- GILMORE, C. J. (1983). *MITHRIL. Structure Solution Package*, Univ. of Glasgow, Scotland.
- HOPFINGER, A. J. (1973). *Conformational Properties of Macromolecules*, Ch. 2. New York: Academic Press.
- KELLER, E. (1984). *SCHAKAL*. Univ. of Freiburg, Federal Republic of Germany.
- KOČIAN, D., HODOŠČEK, M. & HADŽI, D. (1986). *J. Med. Chem.* **29**, 1418–1423.
- MANTEGANI, S., ARCARI, G., CARAVAGGI, A. M. & BOSISIO, G. (1982). US Patent 4 321 381.
- ROBERTS, P. J. & SHELDRIK, G. M. (1975). *XANADU*. Program for crystallographic calculations. Univ. of Cambridge, England.
- SHELDRIK, G. M. (1976). *SHELX76*. Program for crystal structure determination. Univ. of Cambridge, England.
- TONANI, R., DUNBAR, J. JR, EDMONSTON, B. & MARSHALL, G. R. (1987). *J. Comput. Aided Mol. Des.* **1**, 121–132.
- WATERBEEMD, H. VAN DE, CARRUPT, P.-A. & TESTA, B. (1985). *Helv. Chim. Acta*, **68**, 715–723.
- WEINSTEIN, H., CHOU, D., KANG, S., JOHNSON, C. L. & GREEN, J. P. (1976). *Int. J. Quantum Chem. Biol. Symp.* **3**, 135–150.

Acta Cryst. (1989). **C45**, 1044–1047

The Structure of the 1/1 Molecular Complex of Acridine with 1,2,4,5-Benzenetetracarbonitrile

BY L. TOUPET

Groupe de Physique Cristalline, UA au CNRS n° 040804, Université de Rennes I, Campus de Beaulieu, 35042 Rennes CEDEX, France

A. MINIEWICZ

Institute of Organic and Physical Chemistry, Technical University of Wrocław, Wybrzeże Wyspińskiego 27, 50–370 Wrocław, Poland

AND C. ECOLIVET

Groupe de Physique Cristalline, UA au CNRS n° 040804, Université de Rennes I, Campus de Beaulieu, 35042 Rennes CEDEX, France

(Received 1 June 1988; accepted 28 April 1989)

Abstract. $C_{10}H_2N_4 \cdot C_{13}H_{10}N$, $M_r = 367.4$, triclinic, $P1$, $a = 7.447$ (4), $b = 7.885$ (5), $c = 8.072$ (9) Å, $\alpha = 73.93$ (9), $\beta = 84.59$ (9), $\gamma = 85.85$ (6)°, $V = 452$ (1) Å³, $Z = 1$, $D_x = 1.35$ Mg m⁻³, $\lambda(\text{Mo } K\alpha) = 0.71073$ Å, $\mu = 0.078$ mm⁻¹, $F(000) = 194$, $T = 293$ K, $wR = 0.042$ for 1241 observations. The donor molecule does not lie symmetrically above the acceptor. Some of the bond lengths in the acridine molecule do not agree with expected values. This is due to disorder in the acridine–TCNB complex. The mean interplanar spacing between acridine and TCNB is 3.48 (9) Å, which is in agreement with that in similar compounds.

Introduction. Molecular charge-transfer (CT) complexes have recently received a great deal of attention. The crystal structures of most of them exhibit quasi-

one-dimensional stacking. In many structural studies evidence of large anisotropic thermal motions and/or disorder has been found and considerable effort has gone into establishing the important parameters regarding the motion and disorder (Luty & Kuchta, 1986; Boeyens & Levendis, 1984, 1986; Tsuchiya, Marumo & Saito, 1972). Molecular and crystal disorder is important because it influences most of the solid state properties, including energy and charge transport.

This acridine–TCNB complex should in principle be similar (in structural aspect) to the complex of anthracene–TCNB, because acridine is a nitrogen analog of anthracene. Much data has been collected on the anthracene–TCNB complex. Its structure has been studied by X-ray diffraction (Tsuchiya, Marumo & Saito, 1972; Stezowski, 1980), electron para-